SUPPLEMENTAL FIGURES

A

FA013

Chr 6

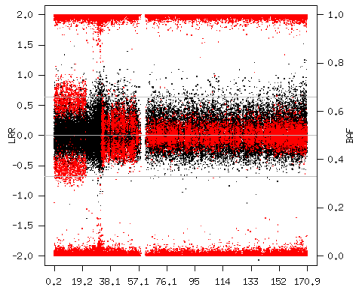

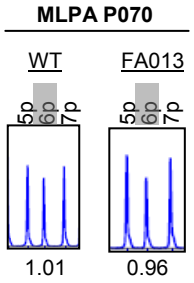

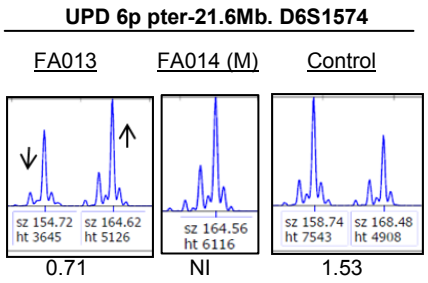

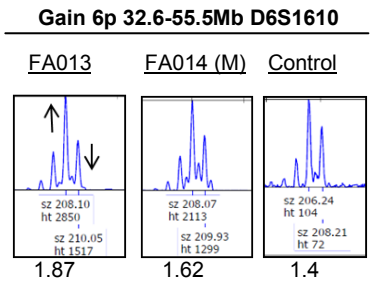

FA072

Chr 1

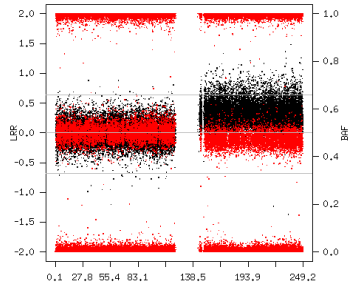

Chr 3

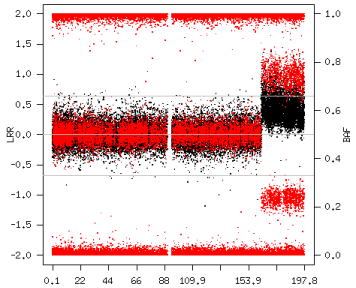

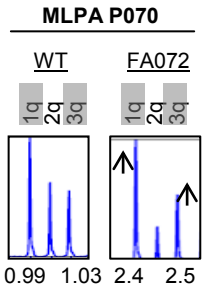

Chr 6

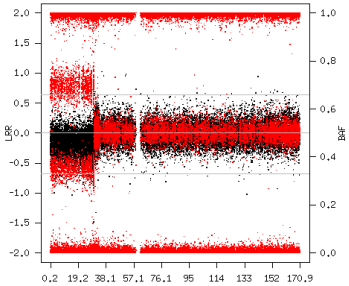

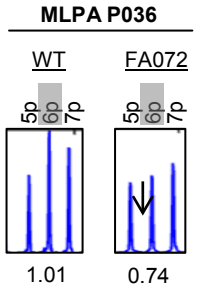

Chr 16

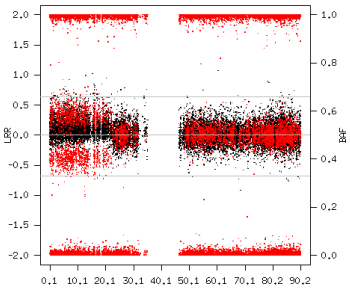

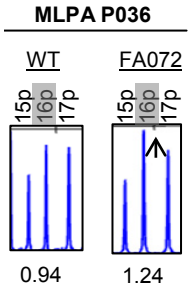

FA117

Chr 10

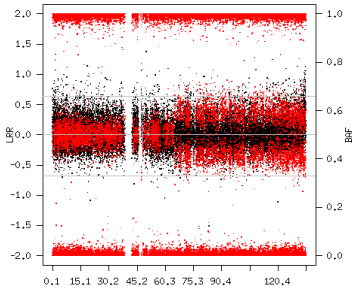

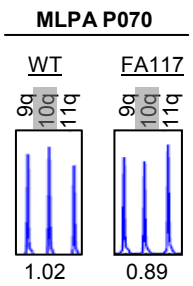

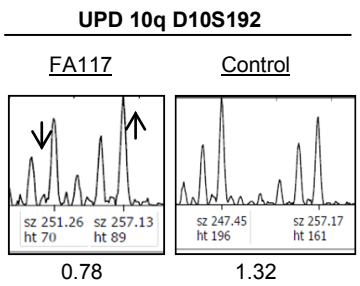

B

FA351

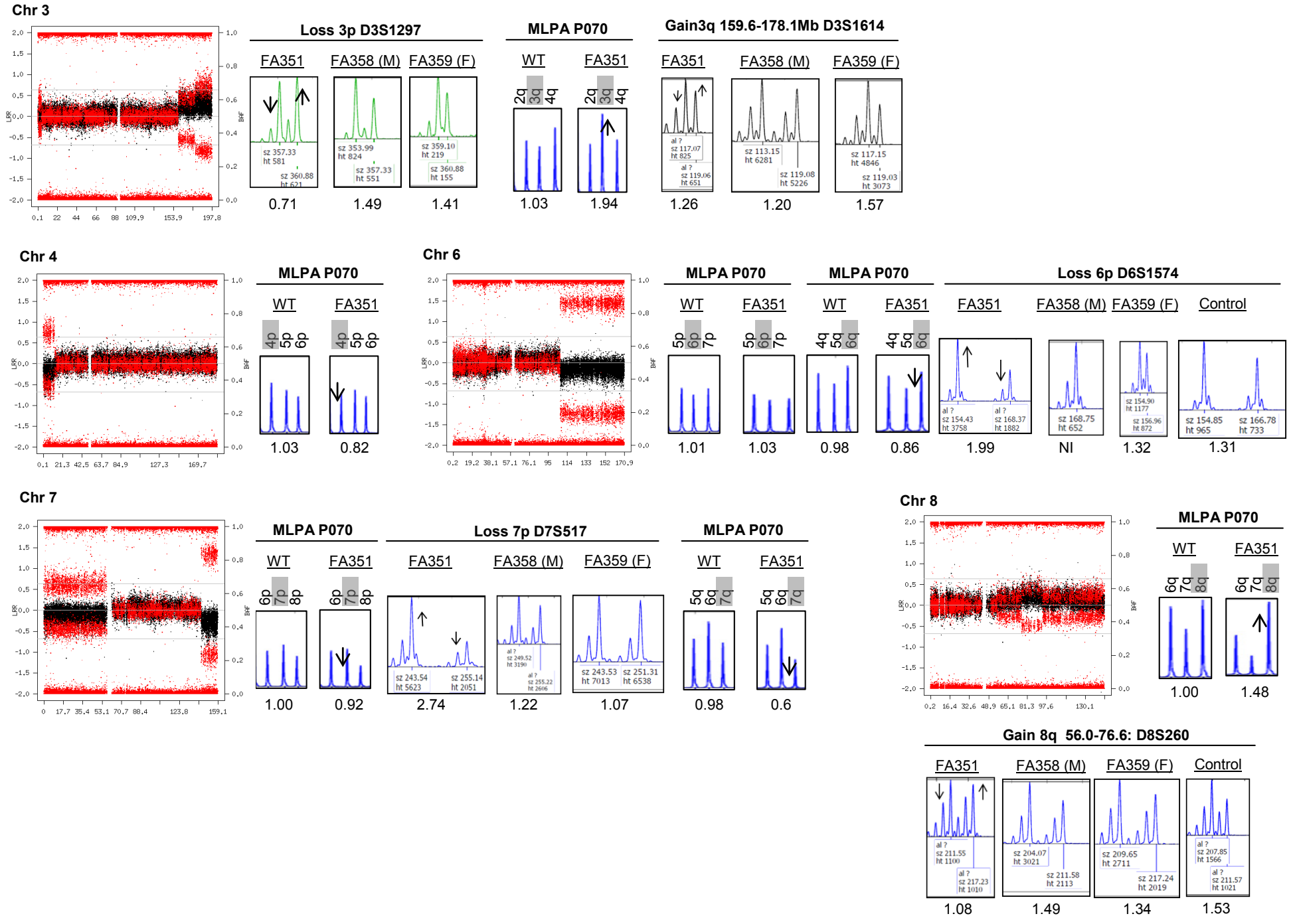
Chr 3
Loss 3p D3S1297
FA351
FA358 (M)
FA359 (F)
0.71
1.49
1.41
MLPA P070
WT
FA351
2q 3q 4q
1.03
1.94
Gain3q 159.6-178.1Mb D3S1614
FA351
FA358 (M)
FA359 (F)
1.26
1.20
1.57
Chr 4
MLPA P070
WT
FA351
4p 5p 6p
1.03
0.82
Chr 6
MLPA P070
WT
FA351
5p 6p 7p
1.01
1.03
MLPA P070
WT
FA351
4q 5q 6q
0.98
0.86
Loss 6p D6S1574
FA351
FA358 (M)
FA359 (F)
Control
1.99
NI
1.32
1.31
Chr 7
MLPA P070
WT
FA351
6p 7p 8p
1.00
0.92
Loss 7p D7S517
FA351
FA358 (M)
FA359 (F)
2.74
1.22
1.07
MLPA P070
WT
FA351
5q 6q 7q
0.98
0.6
Chr 8
MLPA P070
WT
FA351
6q 7q 8q
1.00
1.48
Gain 8q 56.0-76.6: D8S260
FA351
FA358 (M)
FA359 (F)
Control
1.08
1.49
1.34
1.53

C

FA351

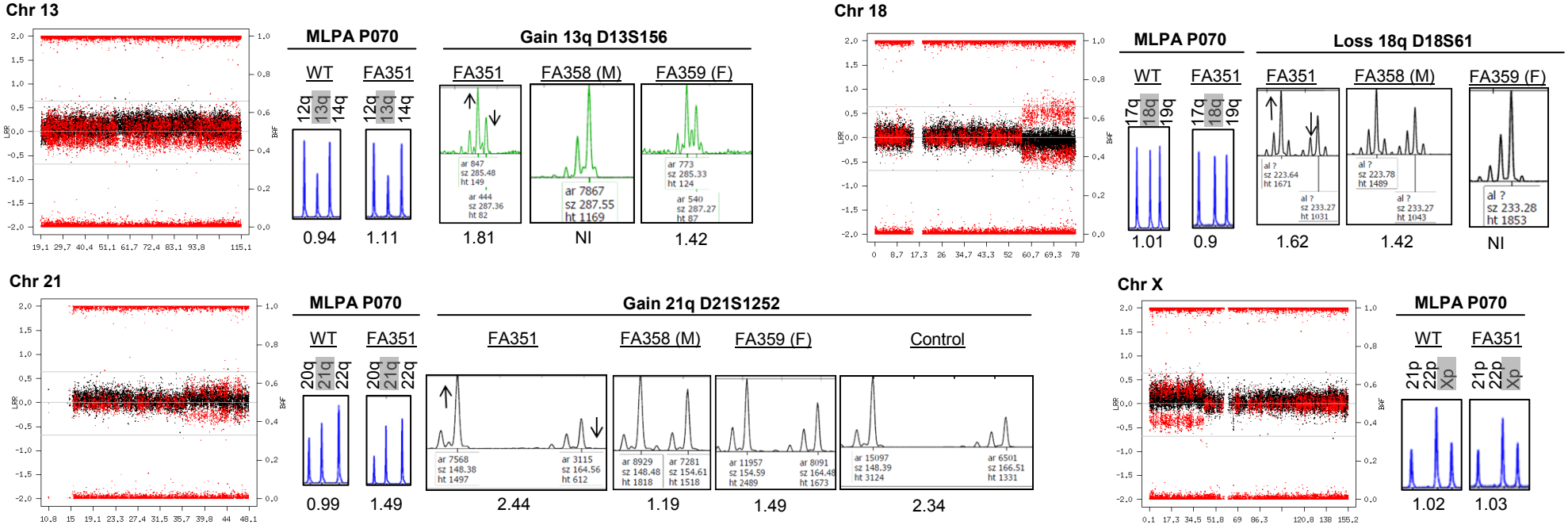

FA360

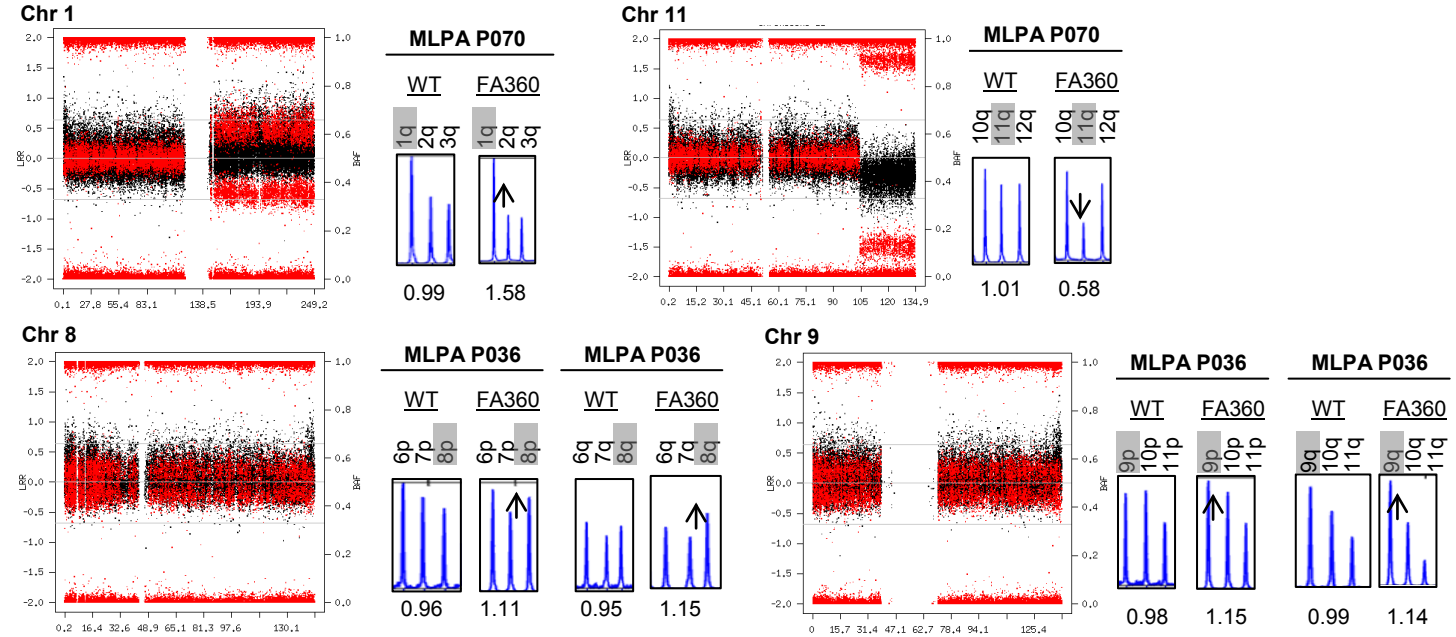

D

FA466

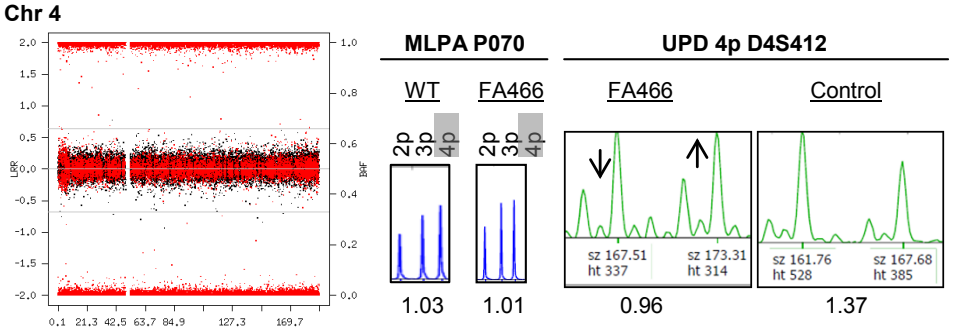

110243

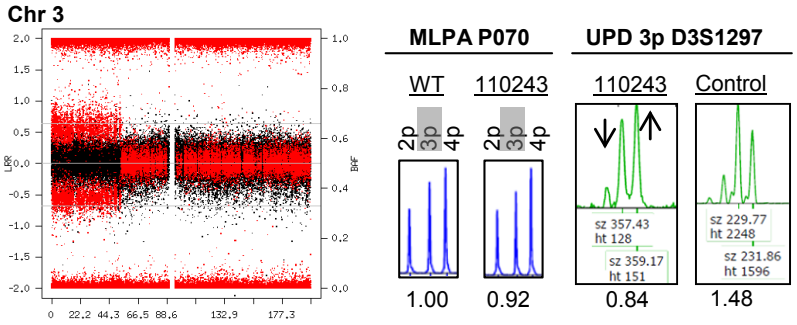

FA647

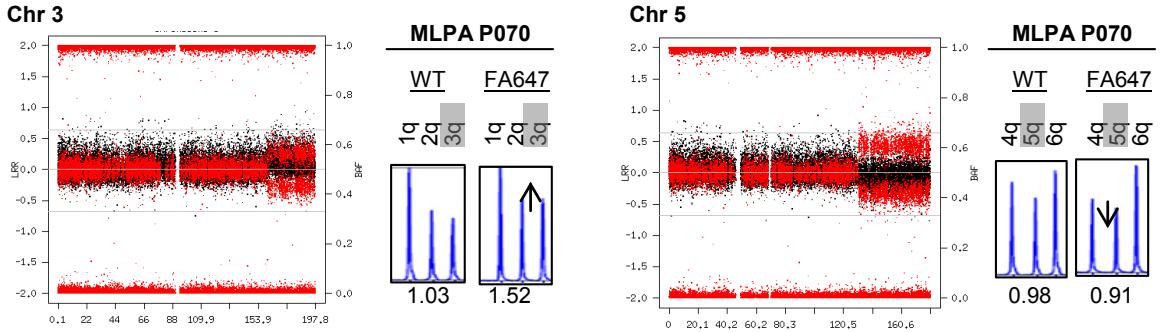

FA648

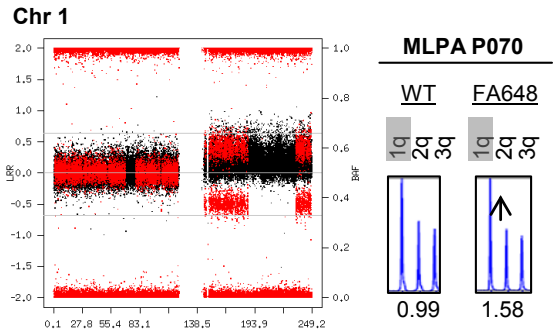

EGF058

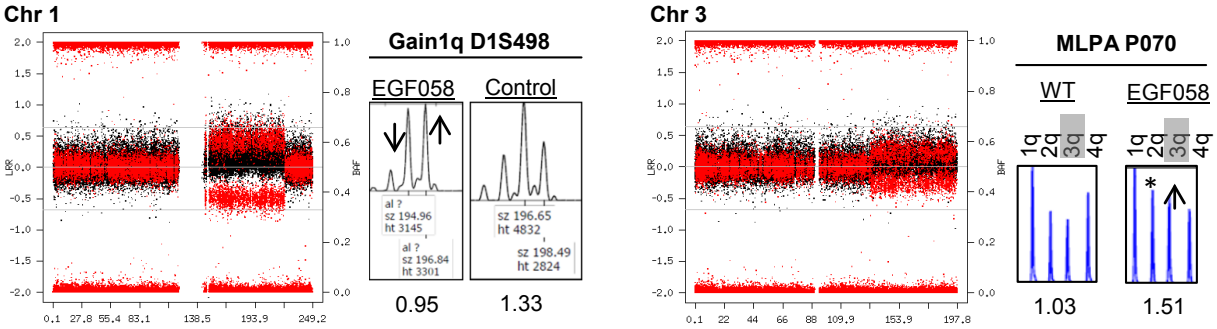

E

041607

Chr 7

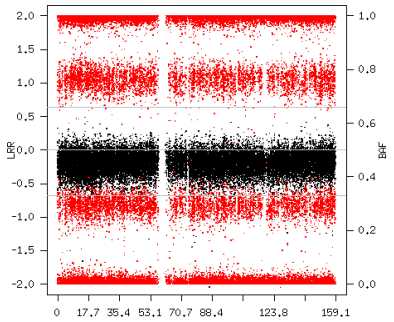

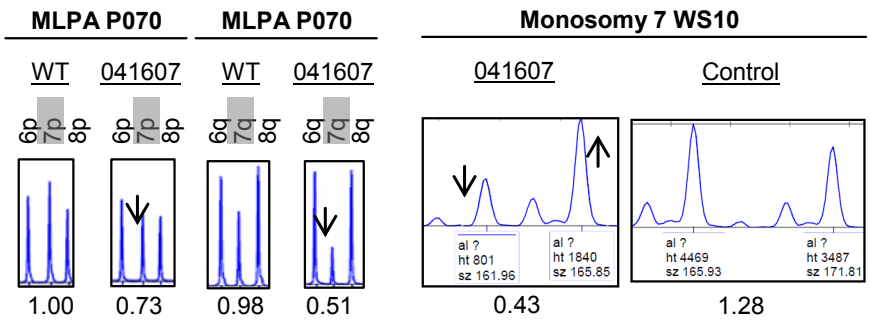

000644

Chr 7

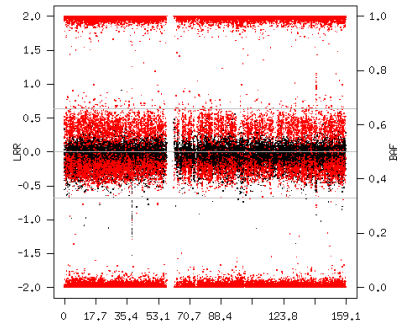

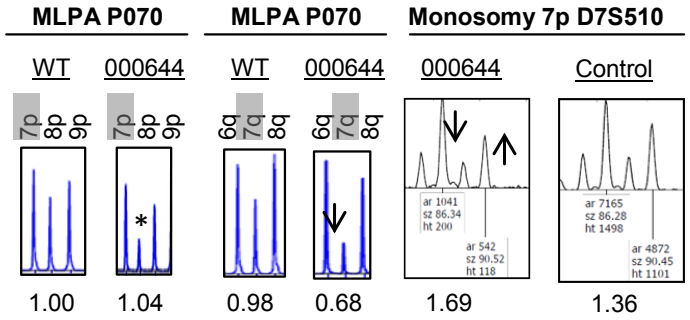

Chr 12

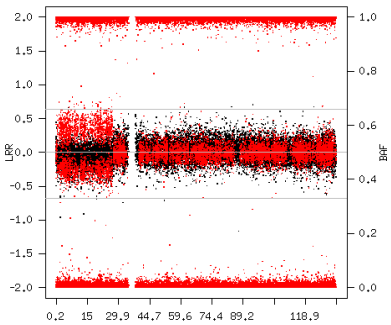

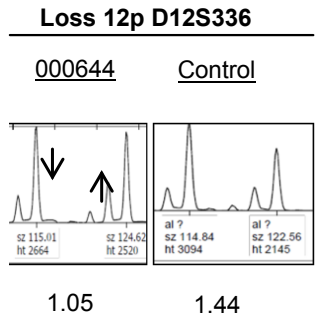

Chr 20

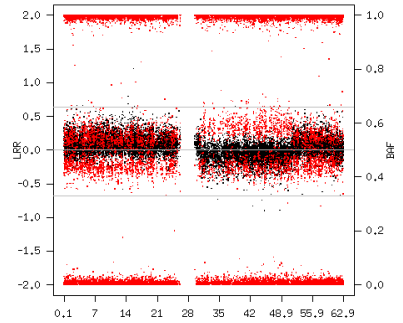

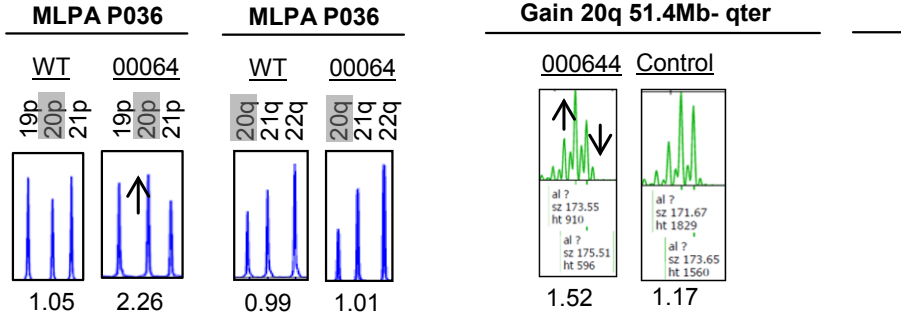

F **041869**

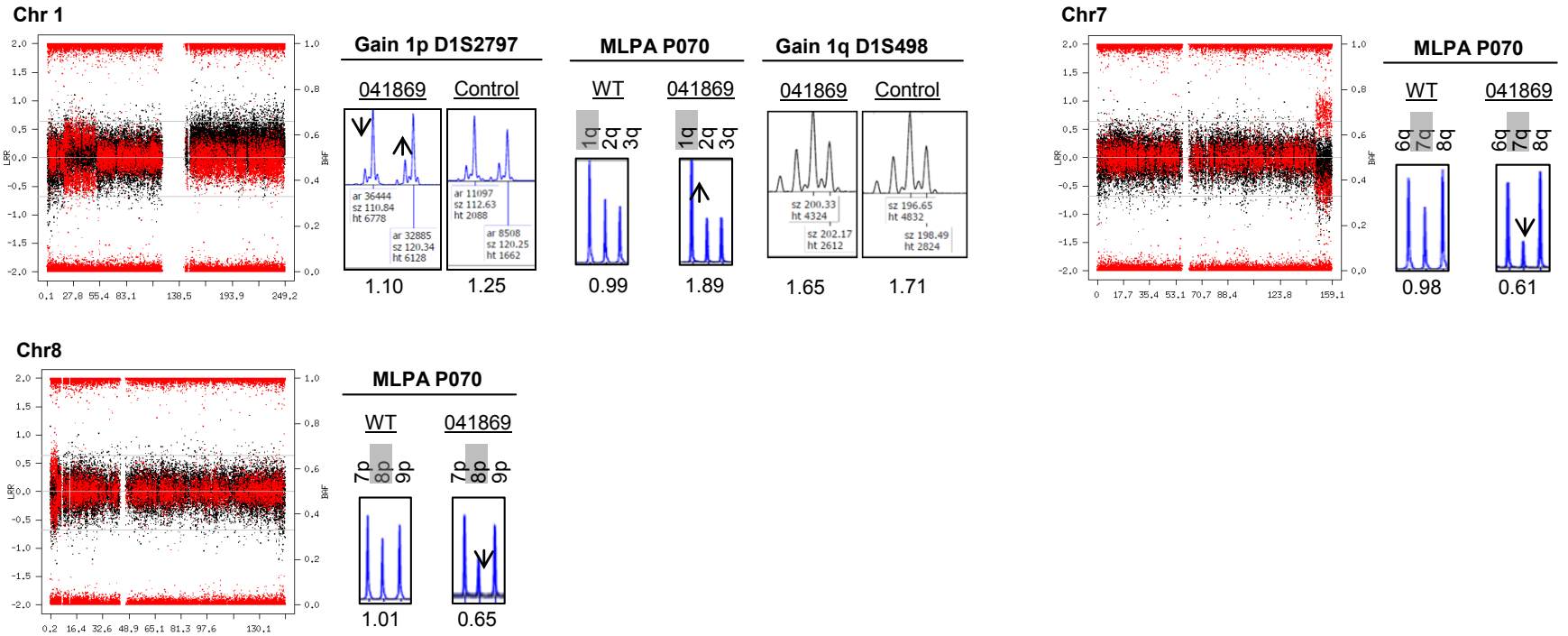

Figure S1. SNP array plots and additional experimental validation of mosaic chromosomal rearrangements detected in FA patients. SNP array plot images show the LogR ratio (LRR) indicated with black dots (scale on the left side) and B-allele frequency (BAF) indicated with red dots (scale on the right side). LRR is a measure of relative probe intensity ratio and provides copy number data whereas BAF is an estimation of the frequency of the B allele of a given SNP in the cell population used for validations. LRR and BAF in combination were used to distinguish between normal cells (BAF at any locus is either 0 (AA), 0.5 (AB) or 1 (BB) and LRR is 0) from copy-number changes (LRR and BAF are altered) and copy-neutral changes as UPDs (LRR is 0 and BAF is altered). Experimental validations were performed on the same source of DNA used for the SNP array by MLPA (P070/P036 panels, all subtelomeric probes) to measure dosage, and/or microsatellite analysis to measure allelic balance. **Table S1** shows the genome coordinates (hg19 assembly) for the microsatellite markers and MLPA probes.

A) FA013: UPD 6p, gain 6p; FA072: gain 1q, gain 3q, loss 6p, gain 16p; FA117: UPD 10q. MLPA confirmed the disomic state at loci with UPDs (~1.0 RPH) as well as the gains (>1.0 RPH) and losses (<1.0 RPH) of genetic material in cases with subtelomeric CNVs rearrangements. Microsatellite analysis showed the expected allelic imbalance in all tested cases reflected by an abnormal ratio between allelic peaks (arrows) compared to the wild type (WT) pattern. In FA013, MLPA 6p probe is testing terminal UPD 6p.

B) FA351: loss 3p, gain 3q (159.6-178.1Mb, 178.1Mb-qter), loss 4p, loss 6p and 6q, loss 7p and 7q, gain 8q (56.0-76.6Mb, 76.6-93.6Mb, 94.2Mb-qter). MLPA confirmed the gain or loss of genetic material in all tested regions except for loss 6p. However, all mosaic rearrangements studied by microsatellite analysis had an allelic imbalance, including loss 6p. Gain 8q 76.6-93.6Mb could not be tested by MLPA because of its interstitial location neither microsatellite analysis since we had no available microsatellite to be tested in this region. In FA351, MLPA 3q probe is testing gain 3q 178.1Mb-qter and MLPA 8q probe is testing gain 8q 94.2Mb-qter.

C) FA351: gain 13q, loss 18q, gain 21q, gain Xp; FA360: gain 1q, loss 11q, trisomies in chromosomes 8 and 9. No enough robust MLPA RPH values were obtained compared to WT ones for FA351 rearrangements, however gain 13q and loss 18q were validated with the detection of abnormal allele peak ratios in microsatellite analysis.

Gain 21q had unclear allele peak ratios whereas gain Xp could not be tested with this approach since we had no available microsatellite to be tested in this region. In FA360, MLPA was enough to ratify all genetic material gains and losses.
D) FA466: UPD 4p; 110243: UPD 3p; FA647: gain 3q, loss 5q; FA648: gain 1q; EGF058: gain 1q, gain 3q. As expected, abnormal peak ratios were obtained in microsatellite analysis in all tested cases as well as MLPA revealed the disomic state for UPDs and gains and losses of genetic material in copy number variations (CNVs). However, in FA647, the loss of genetic material in 5q is not enough marked. In EGF058, MLPA 2q probe was altered (asterisk) but an increased 3q peak could be seen when it is compared with 1q and 4q peaks in EGF058 versus WT pattern. Gain 1q in EGF058 could not be analyzed by MLPA since it is an interstitial rearrangement.
E) 041607: monosomy 7; 000644: monosomy 7, loss 12p, gain 20p, loss 20q cen-51.4Mb, gain 20q 51.4Mb-qter. MLPA confirmed the gain or loss of genetic material in all tested regions except for 000644 monosomy only at 7p. However, all mosaic rearrangements studied by microsatellite analysis had an allelic imbalance, including 000644 monosomy 7p. In 000644, MLPA 8p probe was altered (asterisk) but no reduced 7p peak could be seen when it is compared with 9p peak in 000644 versus WT pattern. Gain 20q 51.4Mb-qter could not be demonstrated by MLPA.
F) 041869: gain 1p, gain 1q, loss 7q, loss 8p. MLPA revealed the gain and losses of genetic material in all tested cases. Gain 1p could not be tested by MLPA because of its interstitial location but imbalanced allele ratio in microsatellite analysis verified this rearrangement.
Chr: chromosome; UPD: uniparental disomy; M: mother; F: father; WT: wild type.

High resolution SNP array (1M/730K)

Low resolution SNP array (250K)

FA013

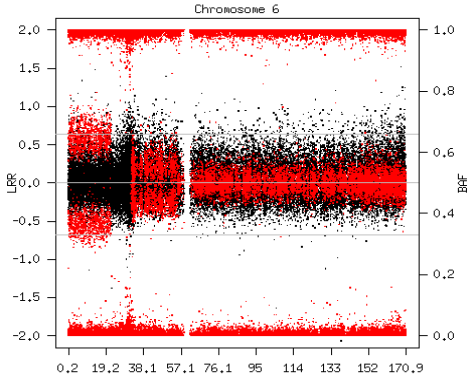

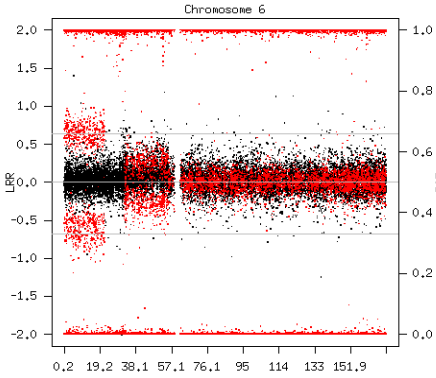

FA072

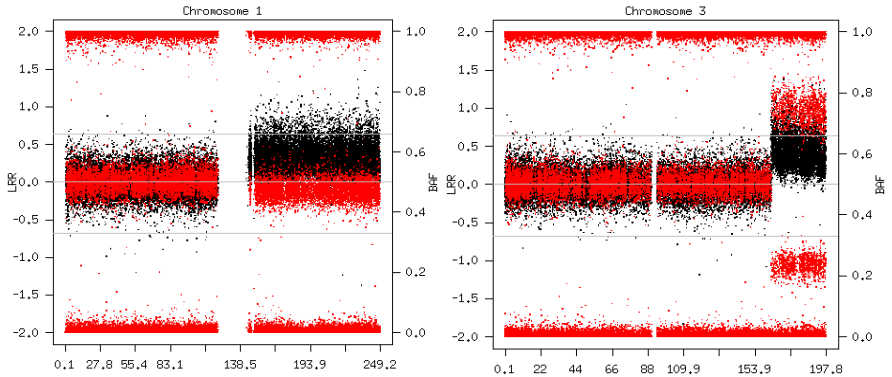

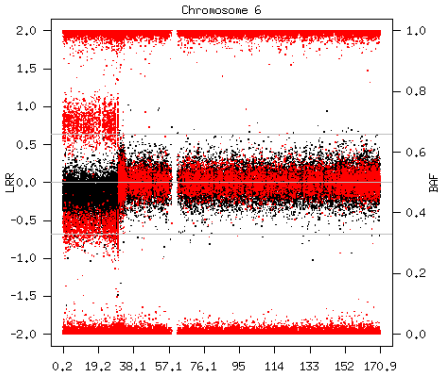

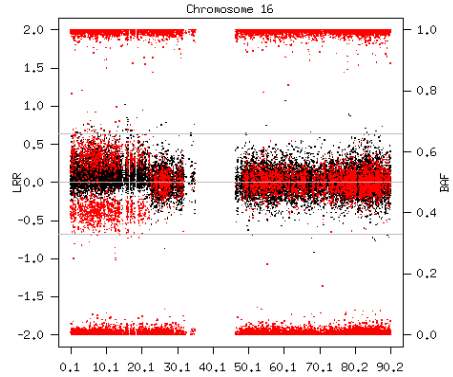

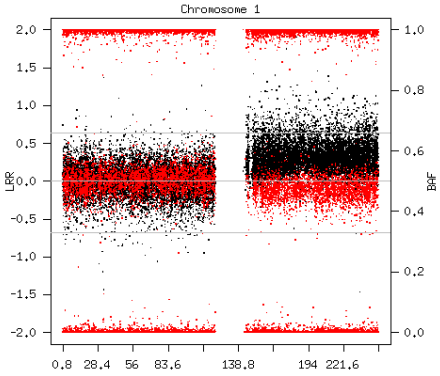

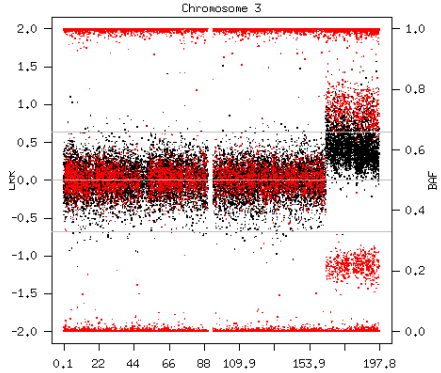

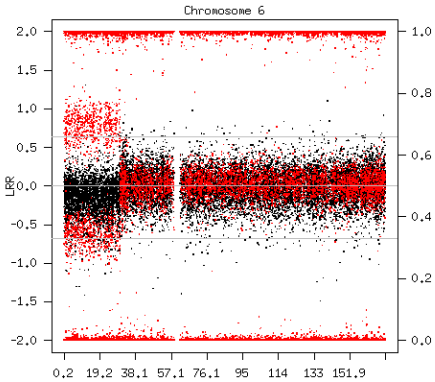

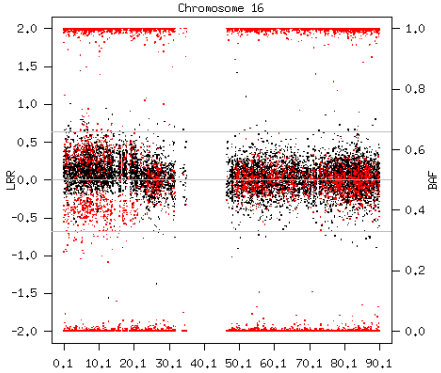

High resolution SNP array (1M/730K)

Low resolution SNP array (250K)

FA117

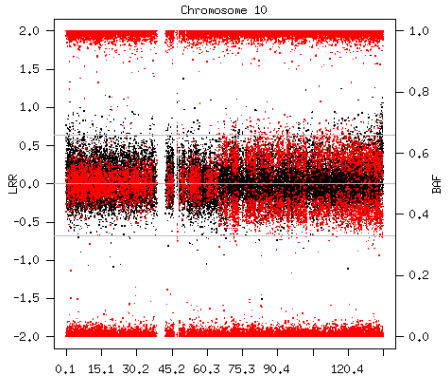

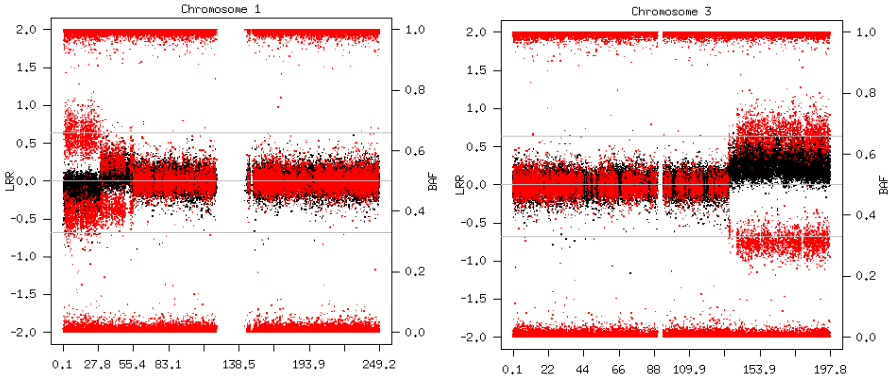

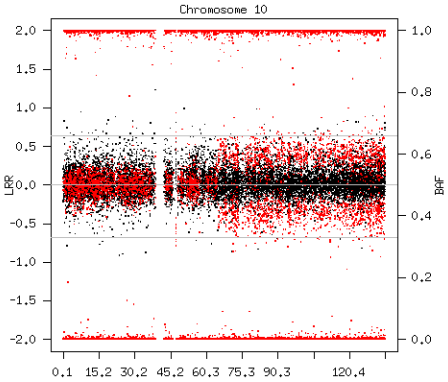

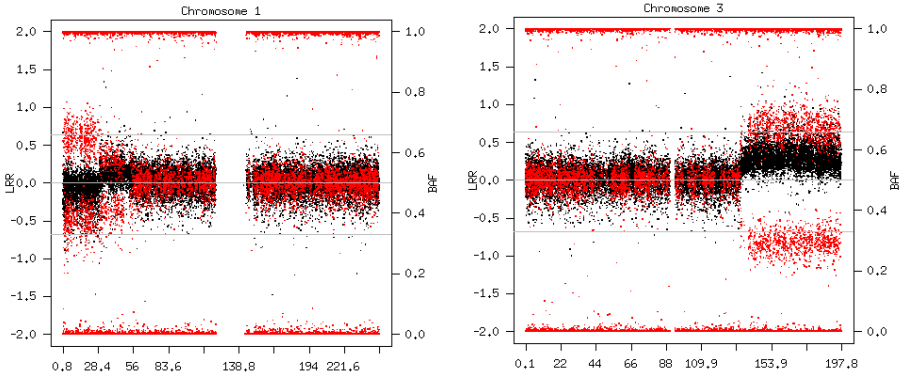

FA178

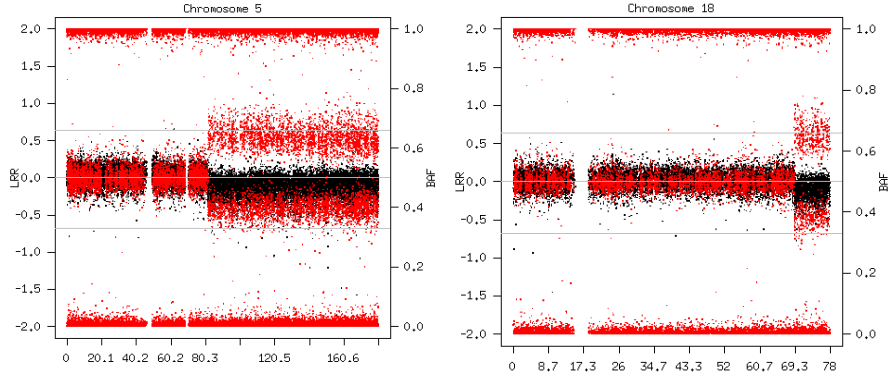

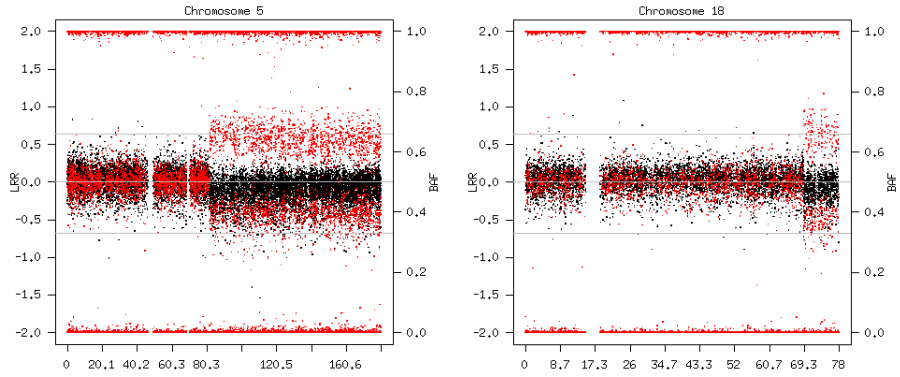

High resolution SNP array (1M/730K)

Low resolution SNP array (250K)

FA351

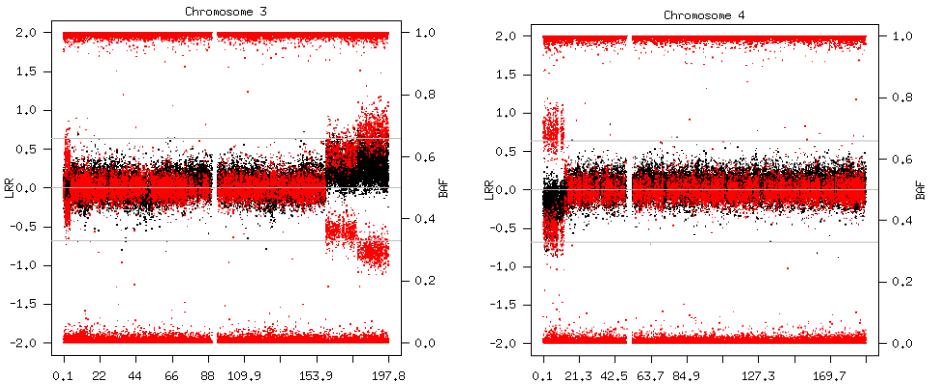

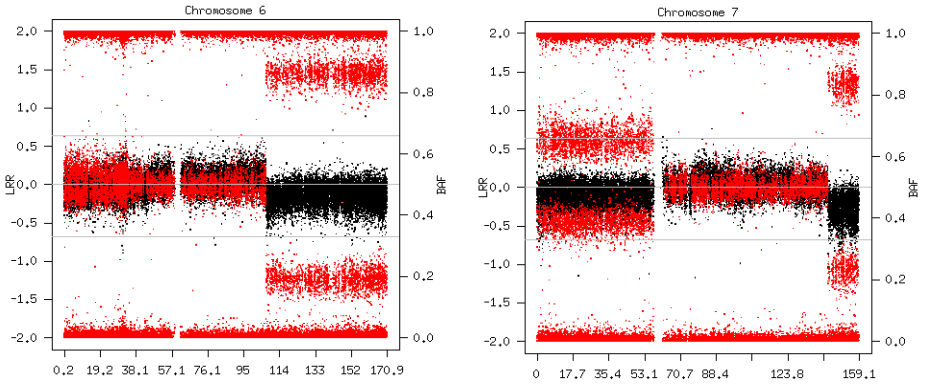

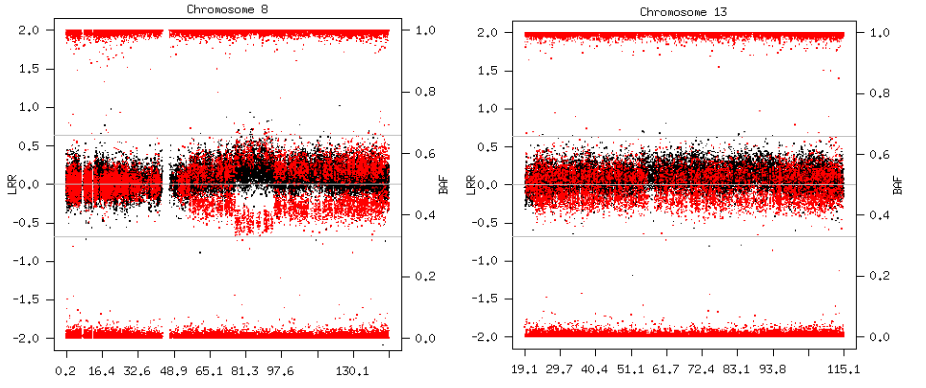

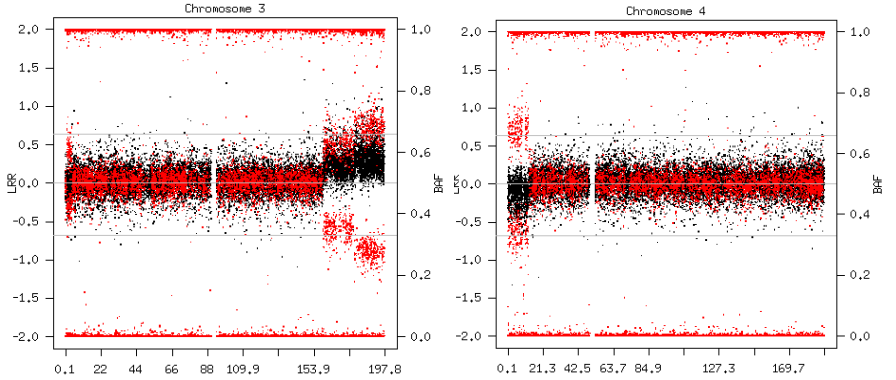

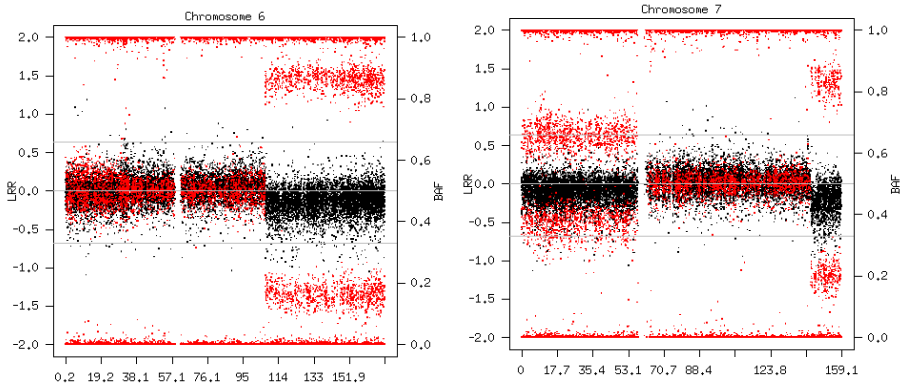

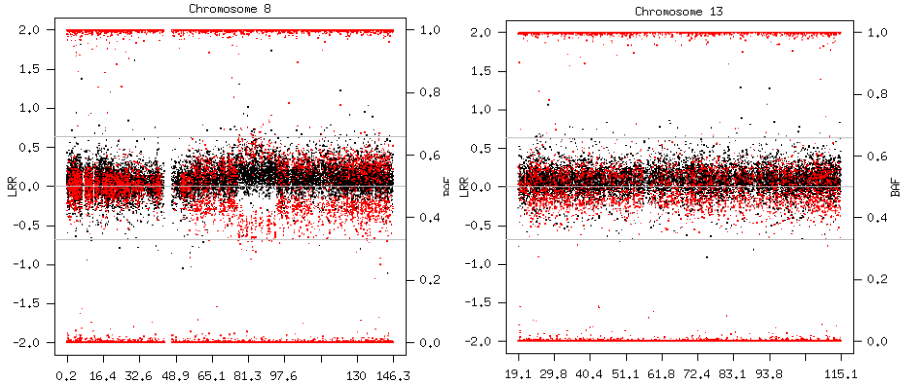

High resolution SNP array (1M/730K)

Low resolution SNP array (250K)

FA351

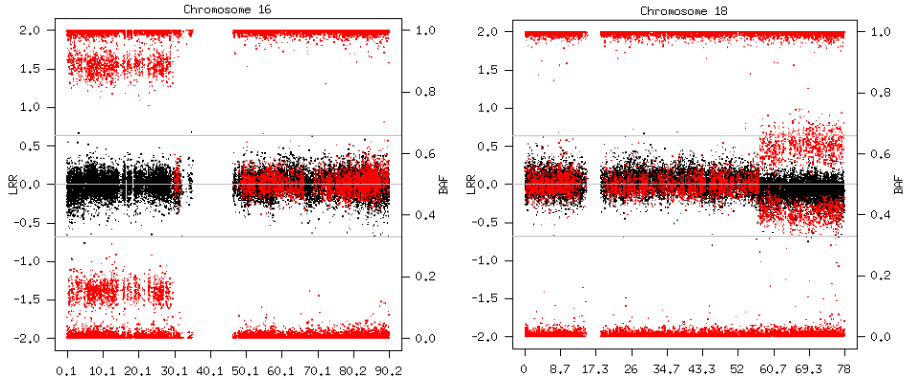

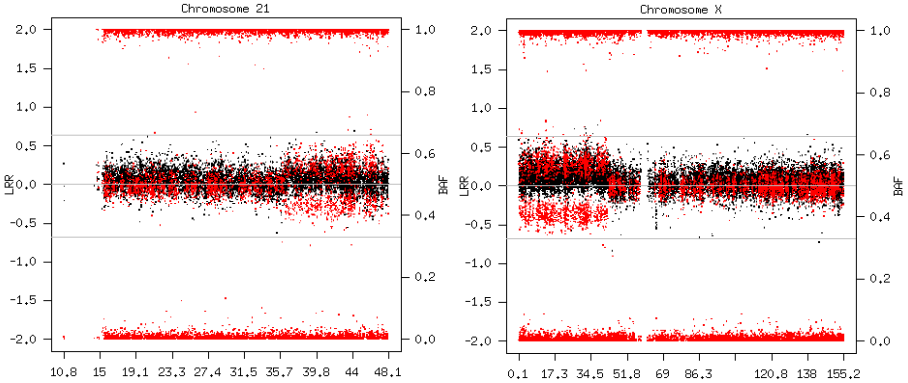

FA360

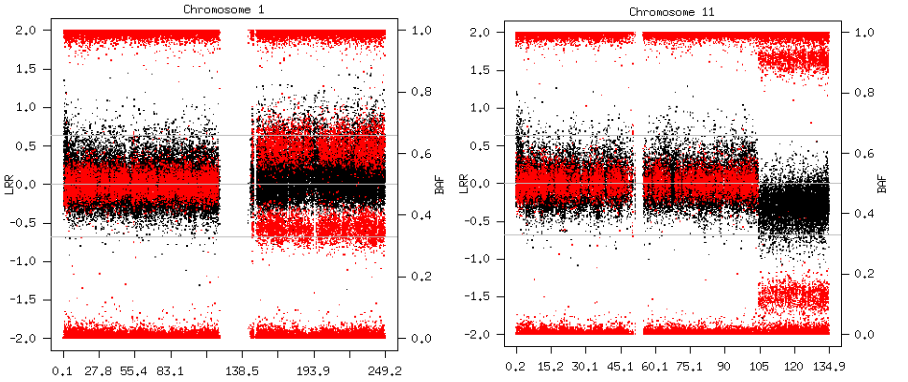

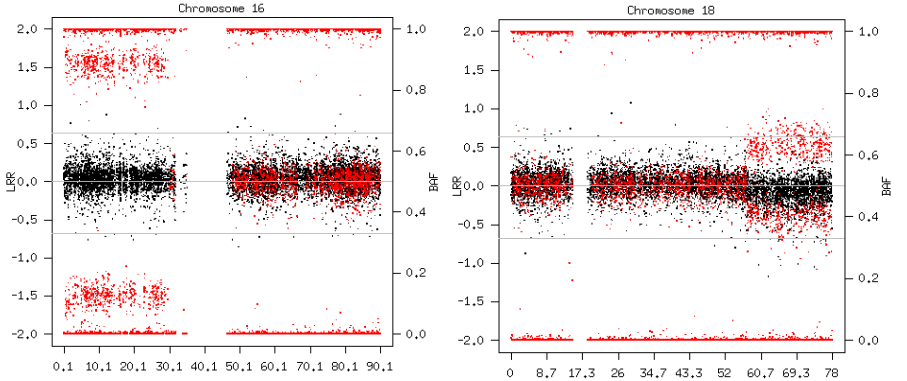

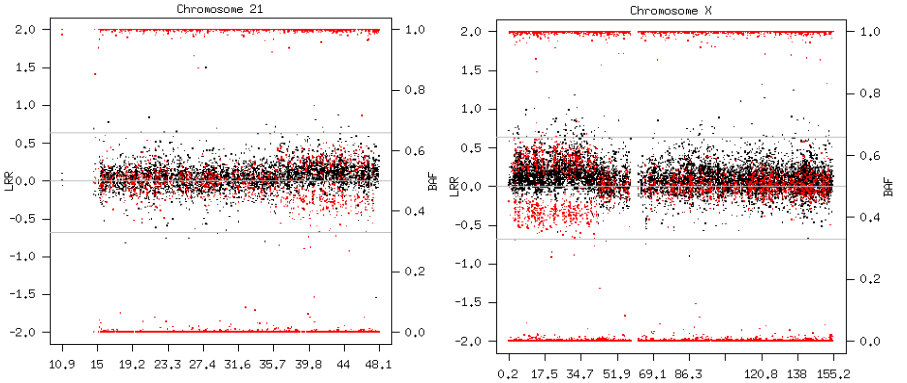

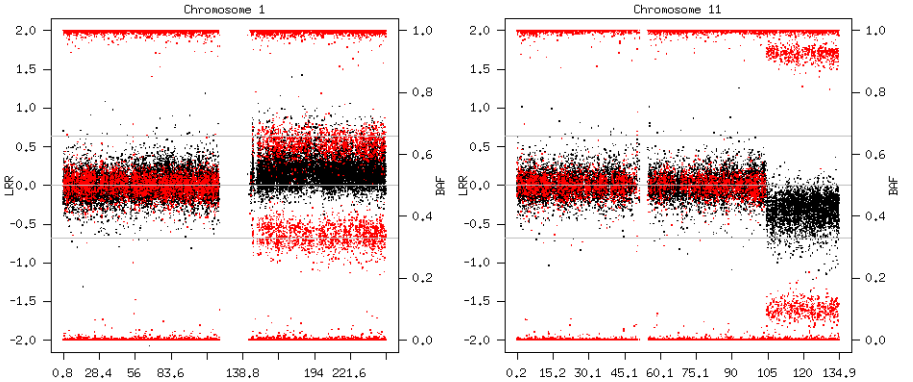

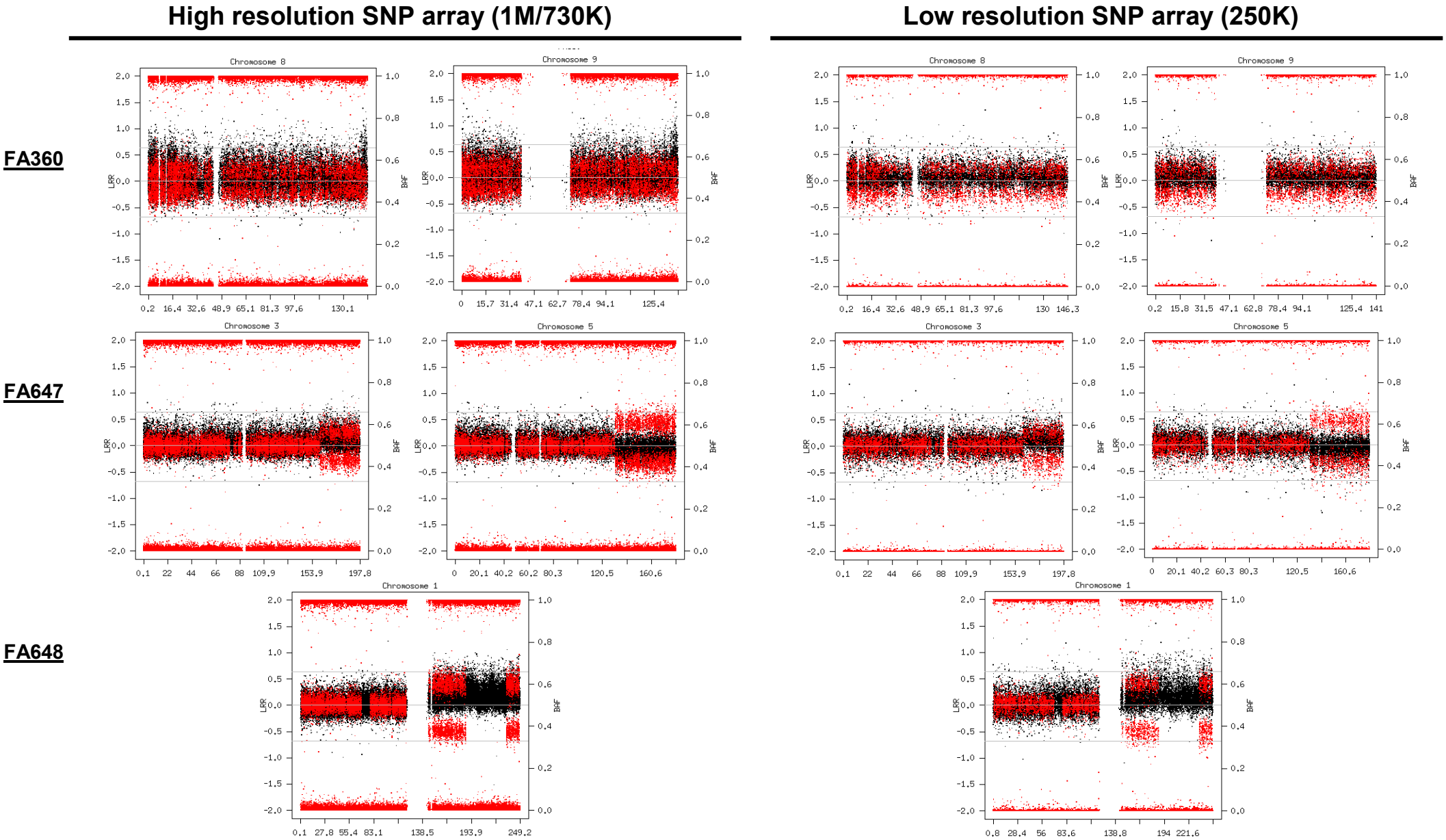

Figure S2. Mosaic rearrangements of 9 FA patients tested by two SNP arrays with different resolution. Samples of 9 FA patients with mosaic rearrangements detected by a high resolution SNP array (1M or 730K) where studied again in a lower resolution SNP array (250K). All mosaic events initially found were also detected with the second approach.

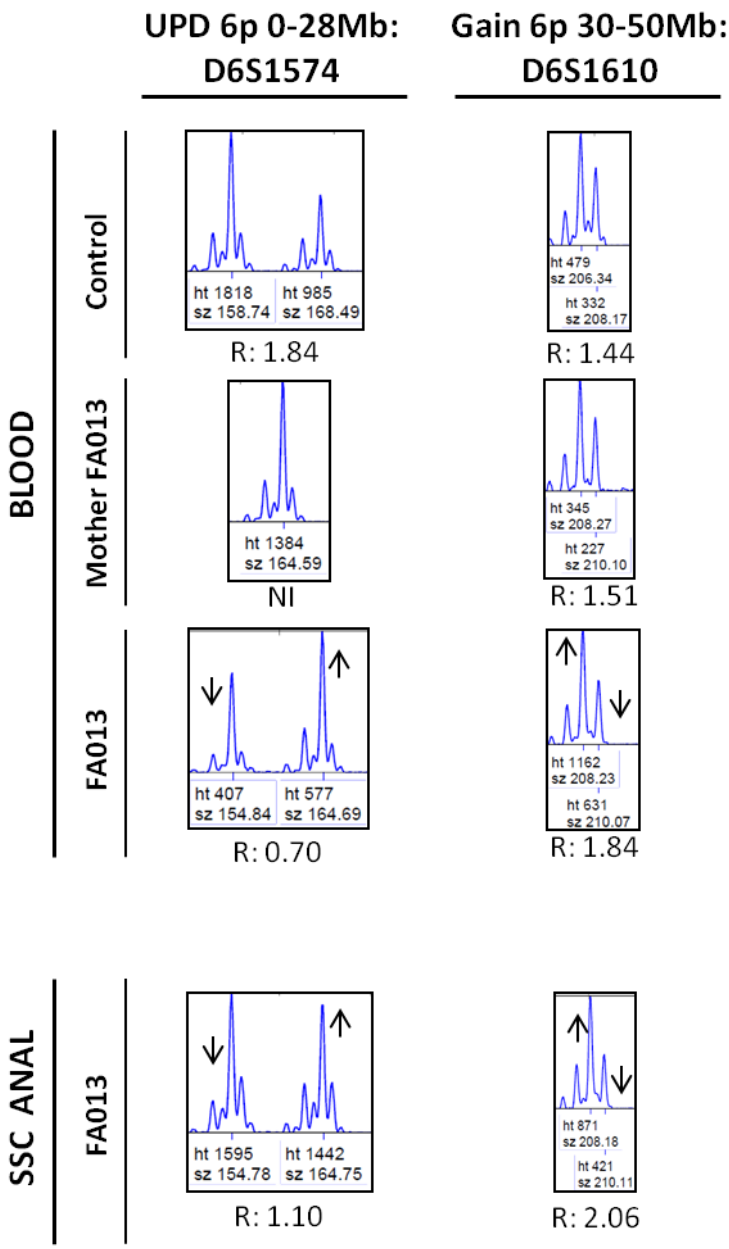

Figure S3. CMEs (distal 6p UPD and proximal 6p gain) detected in peripheral blood of FA013 were also found in an anal SCC developed 10y later.
Microsatellite analysis on blood and tumor DNA in FA013 showed an allelic imbalance in both samples reflected by an abnormal allelic peak ratio (arrows) compared to the WT pattern (controls). The data revealed allelic imbalances consistent with SNP array results interpreted as an UPD at distal 6p (0-28Mb) and a gain at proximal 6p (30-50Mb). In the SSC anal sample, the allelic imbalances were also detected by both microsatellites (proximal and distal) but the relative proportions were different from those in blood. This finding suggests that an initial rearrangement occurred early in embryogenesis in a cell precursor of both tissues, with subsequent independent clonal progression. Unfortunately, SNP array data could not be collected from tumor DNA for further analysis due to technical problems.

SUPPLEMENTAL TABLES

Table S1. Interpretation and raw-data of the SNP array and additional experimental validations of 51 mosaic chromosomal rearrangements detected in 16 out of 130 FA patients. Blood DNA was analyzed by HumanOmniExpress-12 v1-1SNP array 1M (n=1, labeled by +) or 730K (n=15, labeled by ++). From column 1 to 7, this table indicates the FA patient ID with detected clonal mosaicism, the type of rearrangement, chromosome location, start and end chromosome coordinates, size and estimated percentage of cells affected (% of mosaicism). Detection of mosaic rearrangements was based on MAD analysis using log R ratio (LogR) and B-allele frequency (BAF). LogR is a measure of the relative probe signal intensity and provides data on copy number whereas BAF estimates the frequency of the B allele of a given SNP in a sample. In cells without chromosomal rearrangements, we expect to detect BAF values of 0 (AA), 0.5 (AB) or 1(BB) at any locus and LogR near 0. Copy-number and copy-neutral changes will alter BAF, and only copy-number changes will also affect LogR. The difference between the observed and expected BAF is denoted as b-deviation (Bdev), thus, altered regions can be called by detecting segments with b-deviation values different from zero. In this table (from column 8 to 14 microarray data is shown for each sample: *LogR sample* is the LogR from all autosomal probes (chr1-22) of the array in each sample; *Log R chr* is the LogR from all probes of the chromosome analyzed; *Log R mosaic* is the LogR from all probes within the rearranged region; *LogR mosaic adjusted* is the LogR mosaic adjusted by the autosomal average LRR (LogR sample) in samples with only one mosaic event or by the average LRR in a region of the same chromosome without events in samples with more than one rearrangement. *BdevHet sample* is the B-deviation from all autosomal heterozygous probes in each mosaic sample (chr1-22); *BdevHet chr* is the B-deviation from all heterozygous probes of the chromosome analyzed; *BdevHet mosaic* is the B-deviation from all heterozygous probes within the rearranged region.
Experimental validations (MLPA and microsatellite analysis) were performed on the same source of DNA used for the SNP array. MLPA (P070/P036 panels) was carried out to analyze dosage (copy-number versus copy-neutral) at all subtelomeric regions, whereas microsatellites analyzed allelic balance. From column 14 to 19, this table shows MLPA probes used in each case together with their chromosome location and their starting and ending point. MLPA results are also shown for controls and tested samples confirming the disomic state at loci with UPDs (~1.0 RPH) in 4 out of 4 cases, the gain of genetic material (>1.0 RPH) in 16 out of 17 cases and the loss of genetic material (<1 RPH) in 11 out of 13 tested cases. Microsatellite analysis data is presented in columns 20 to 25. Results showed the expected allelic imbalance in 20 out of 21 tested cases reflected by an abnormal ratio between allelic peaks compared to the wild type (WT) pattern. There was a single rearrangement with discordant experimental validation (failure to detect Xp gain by MLPA in FA351). In total, 9 rearrangements from FA178 (5), FA351 (3) and FA106 (1) could not be tested because of technical problems.
ID: identification; Chr: chromosome; bp: base pair; pter: p terminal; qter: q terminal; cen: centromere; UPD: uniparental disomy; NA (I): not analyzed because interstitial location; NA (D): not analyzed because no DNA available; NI: not informative (homozygous marker); C: control; F: father; M: mother; R: ratio between allele peaks in microsatellite analysis. * Tetrasomy; ** Possible translocation; *** Complex rearrangement. All genomic coordinates are in hg19 assembly.

Table S2. Interpretation and raw-data of the SNP array of 30 mosaic chromosomal rearrangements detected in 29 controls. This table includes information as the estimated age at sampling, the study and the SNP array platform used about the control individuals in whom mosaic events were detected.

Table S3. Features of FA patients with no detectable CME at the time of sample collection (114/130). From left to right, the ID of each patient is shown as well as their complementation group, their age at blood sample collection, years from sample collection to the first cancer post-sampling diagnosis and the kind of cancer detected. Evolution is also reported and also the death cause (when required) and the inclusion or not of each individual in the Kaplan-Meier analysis is indicated in the last column. In order to estimate the false negative rate of SNP array as a tool to detect cancer early, we considered that SNP array should detect CMEs in blood of all FA patients with AML/MDS at time of sample collection. In our cohort, there was 1 FA patients with precancerous stage (MDS) at the time of sample collection (011706 with MDS) and no detectable CMEs. (+) patients with reverse mosaicism of the FA mutation in blood; * no information available about the type of cancer; NA: not available; CMEs: chromosomal mosaic events.

Spanish Fanconi Anemia Clinicians's Network		
Surnames, name	**Hospital**	**City**
Arrizabalaga, Beatriz	Hospital de Cruces	Barakaldo
Badell Serra, Isabel	Hospital de la Santa Creu i Sant Pau	Barcelona
Balmaña Gelpi, Judith	Hospital Vall d'Hebrón	Barcelona
Baragaño González, Marta	Hospital San Rafael	Barcelona
Beléndez Bieler, Cristina	Hospital General Univ. Gregorio Marañón	Madrid
Benito Bernal, Ana I.	Hospital Univ.de Salamanca	Salamanca
Bergua Burgués, Juan Miguel	Hospital San Pedro de Alcantara	Cáceres
Blanco Quirós, Ana	Hospital Clínico Universitario de Valladolid	Valladolid
Carrió Ybañez, Anna	Hospital Clínic	Barcelona
Català Temprano, Albert	Hospital Sant Joan de Déu	Barcelona
Couselo Sánchez, José Miguel	Comp.H.Univ. de Santiago de Compostela	Santiago de Compostela
Cuesta Gallardo, Isabel	Hospital Obispo Polanco	Teruel
Dasí Carpio, Mª Angeles	Hospital Universitario La Fe	Valencia
De la Mata Franco, Gregorio	Hospital Univ. De Burgos	Burgos
Díaz de Heredia, Cristina	Hospital Vall d'Hebrón	Barcelona
Fernández Rañada, José Mª	Hospital Severo Ochoa	Leganés (Madrid)
Figuera Álvarez, Ángela	Hospital Univ. La Princesa	Madrid
Fuentes Gutierrez, Inmaculada	Hospital Univ. Infanta Cristina	Parla (Madrid)
Fuster, José Luís	Hospital Infantil Virgen de la Arrixaca	Múrcia
García Bernal, Marta	Hospital Mutua de Terrassa	Terrassa (Barcelona)
García Pardos, Carmen	Hospital Univ. Donostia	San Sebastián
García-Miñaúr, Sixto	Hospital Univ. La Paz	Madrid
González Fernández, Fernando A.	Hospital Clinico de San Carlos	Madrid
Hermosín, Mª Lourdes	Hospital Jerez de la Frontera	Jerez de la Frontera
Hernando, Inés	Hospital Univ. Central de Asturias	Oviedo
López Duarte, Mónica	Hospital Univ. Marqués de Valdecilla	Santander
Marín Iglesias, Rosario	Hospital Univ. Puerta del Mar	Cádiz
Martín Segovia, José Maria	Hospital Montecelo	Pontevedra
Martínez Badas, Mª Paz	Hospital Fundación Alcorcón	Alcorcón (Madrid)
Melero Moreno, Carmen	Hospital 12 de Octubre	Madrid
Molina García, Juan	Hospital Marina Baixa	Alicante
Muñoz Villa, Arturo	Hospital Univ. Ramón y Cajal	Madrid
Navarro Álvarez, Pilar	Hospital Virgen de las Nieves	Granada
Ojeda Gutiérrez, Emilio	Hospital Puerta de Hierro Majadahonda	Majadahonda (Madrid)
Peláez Pleguezuelos, Irene	Hospital Materno Infantil de Jaén	Jaén
Pérez de Soto, Inmaculada	Hospital Infantil Virgen del Rocio	Sevilla
Rodríguez Villa, Antonia	Hospital Reina Sofía	Córdoba
Rosell Andreo, Jordi	Hospital Univ. Son Espases	Palma
Rosiñol Dachs, Laura	Hospital Clínico de Barcelona	Barcelona
Ruiz Sánchez, Pedro L.	Hospital Materno Infantil de Málaga	Málaga
Sánchez Calero, Jesús	Hospital Virgen de la Macarena	Sevilla
Sevilla Navarro, Julián	Hospital Infantil Univ. Niño Jesús	Madrid
Tapia Torres, María	Hospital General de La Palma	Santa Cruz de Tenerife
Vagace Valero, José Manuel	Hospital materno Infantil de Badajoz	Badajoz
Valiente Martín, Alberto	Hospital Virgen del Camino	Pamplona

Table S4. Spanish Fanconi Anemia Clinicians' Network involved in this study. A list of the name of clinicians that have contributed in this study is provided in this table together with the hospital (and city) where they are affiliated.